Some Correlations Between the Thermodynamic and Transport Properties of High Tc Oxides in the Normal State

J. Cooper, J. Loram

Some Correlations Between the Thermodynamic and Transport Properties of High T_c Oxides in the Normal State

J.R. Cooper (*) and J.W. Loram

IRC in Superconductivity, University of Cambridge, Cambridge CB3 OHE, UK

(Received 11 July 1996, received in final form 26 August 1996, accepted 29 August 1996)

PACS.74.72.-h – High T_c-compounds
PACS.74.25.Bt – Thermodynamic properties
PACS.74.25.Fy – Transport properties (electric and thermal conductivity, thermoelectric effects, etc.)

Abstract. — We review some of the systematic patterns in the normal state properties of high temperature oxide superconductors which may help in the search for the pairing mechanism. A recent analysis of thermodynamic properties, namely the conduction electron entropy determined from high resolution specific heat data and the static magnetic susceptibility, both measured for a wide range of closely spaced compositions, yields much information about the effects of hole doping and zinc substitution on the low energy electronic excitations in these compounds. We attempt to correlate this information with the systematic changes observed in the electrical resistivity, Hall coefficient and most notably the thermoelectric power, for which a new scaling property is reported.

1. Introduction

Understanding the microscopic pairing mechanism responsible for superconducting transition temperatures (T_c) as high as 164 K [1] in the layered cuprates is one of the most fascinating open questions in solid state physics. In the last two years many experiments, especially penetration depth [2,3], tunnelling [4] and tricrystal [5] studies, have provided convincing evidence that for these particular compounds the superconducting state has unconventional $d_{x^2-y^2}$ symmetry. This is clearly an important development, especially for understanding various properties of the superconducting state, including high T_c devices. However it is unlikely that it will be sufficient to discriminate between the many different theories of the pairing mechanism that have been proposed in the last ten years. It is generally agreed that for this problem the way forward is to see which theory best accounts for the systematic behaviour of various normal state properties above T_c as a function of composition, temperature, applied magnetic field and pressure. In this paper we summarise some of our recent experimental work in this area, and some related work in the literature, which may help in this intriguing search for the correct pairing mechanism. It is an honour to dedicate this short review to the memory of the outstanding experimental solid state physicist, Professor I.F. Schegolev.

(*) *On leave from:* The Institute of Physics of the University, Zagreb, Croatia
Author for correspondence (e-mail: jrc@cus.cam.ac.uk)

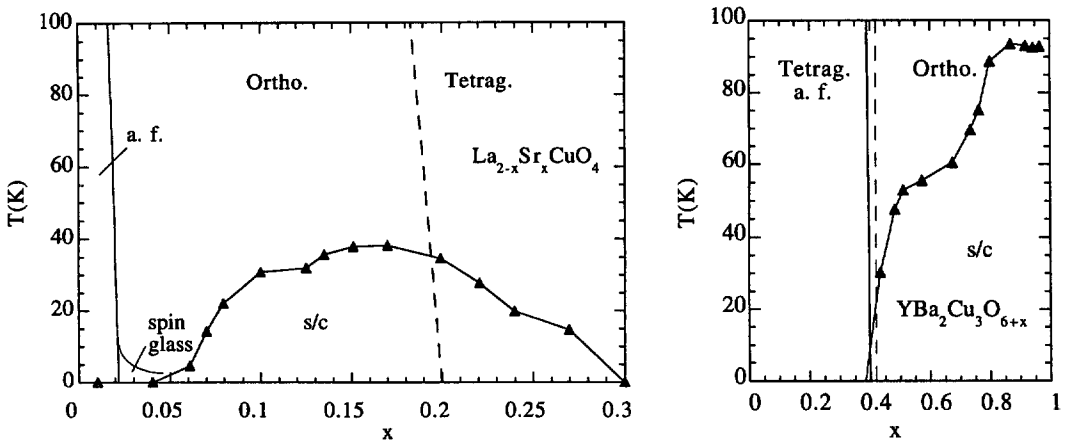

Fig. 1. — Phase diagrams of a) $La_{2-x}Sr_xCuO_4$ [6] and b) $YBa_2Cu_3O_{7-\delta}$ [7]. in both cases the T_c values have been taken from specific heat studies [8, 9].

2. Effects of Hole Concentration on Bulk Transport Properties

The phase diagrams of two of the most widely studied high T_c oxides $La_{2-x}Sr_xCuO_4$ (LSCO) [6] and $YBa_2Cu_3O_{6+x}$ (YBCO) [7] are shown in Figure 1 as a function of Sr and O content respectively, with T_c values determined from specific heat studies [8, 9]. In both cases the superconducting state is induced by adding a small number of holes (p) to each CuO_2 plane. For LSCO it is relatively easy to maintain the oxygen stoichiometry fixed and therefore when La^{3+} is replaced by Sr^{2+} the number of added holes/CuO_2 unit, $p = x$. For YBCO the hole content has been deduced indirectly from bond length analysis (bond valence sums) [10]. It was concluded that the maximum in T_c at 92 K for YBCO corresponds to $p = 0.16$, as for LSCO, but this important point merits further investigation *e.g.* by detailed analysis of Y/Ca substitution experiments. For both YBCO and LSCO relatively small values of p cause a change from the Mott-Hubbard insulating ground state at $p = 0$ to a superconducting ground state. For LSCO the superconducting ground state extends from $x = 0.05$ to 0.27. Surprisingly at higher values of x (*i.e.* p) LSCO remains a good metal but is no longer superconducting.

2.1. Resistivity. — Both compounds continue to become better metals as x is increased, and as shown by the single crystal data in Figure 2 the room temperature conductivity of the CuO_2 planes increases linearly with x for both compounds [11–13] as originally emphasised by Batlogg for polycrystalline LSCO [14]. The typical temperature dependence of the CuO_2 plane resistivity $\rho_{ab}(T)$ is illustrated in Figure 3 for crystalline films of $YBa_2Cu_3O_{7-\delta}$ [11]. The changes in slope above 350 K are thought to arise from oxygen ordering effects [15]. Namely resistivity studies of polycrystalline YBCO samples quenched from 500 – 700 °C into liquid nitrogen show that oxygen atoms in the Cu-O chains (which are disordered because of the quench) quickly develop short range order on warming from 300-320 K but become more disordered again at higher temperatures [15]. Below room temperature, $\rho_{ab}(T)$ is linear in T for $\delta = 0.05$, but for higher values of δ a marked downward curvature sets in below a certain temperature T^*. As discussed by several groups [16–19] this is connected with the spin or normal state gap discussed later in Section 4.1. It is notable that the data in Figure 3 for

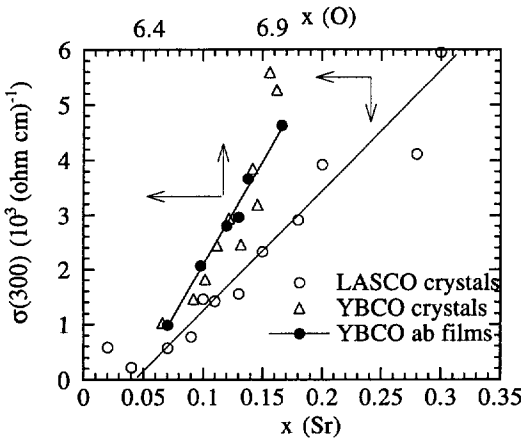

Fig. 2. — Room temperature *ab* plane conductivity of $La_{2-x}Sr_xCuO_4$ crystals, open circles,.[12, 13], $YBa_2Cu_3O_{6+x}$ crystals, open triangles [12, 18] and $YBa_2Cu_3O_{6+x}$ crystalline films, closed circles [11], *versus* Sr content and O content x respectively.

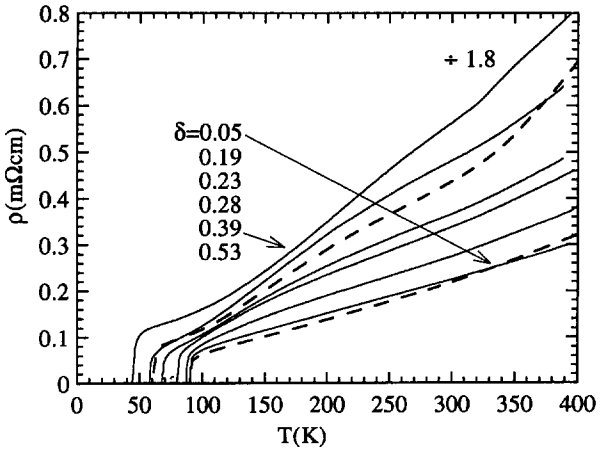

Fig. 3. — Temperature dependence of the *ab* plane resistivities of $YBa_2Cu_3O_{7-\delta}$ crystalline films with the values of δ shown [11]. The dashed lines show data for two single crystals [11] with $\delta = 0$ and 0.4.

YBCO films show a low residual resistivity, almost independent of the oxygen deficiency in the range $0 < \delta < 0.4$. The main effect of reducing the hole concentration is to increase the inelastic (temperature dependent) part of the resistivity by a factor 5. In contrast similar data for polycrystalline samples in Figure 4 [11, 20] show the same general behaviour but a much larger residual resistivity which almost certainly arises from grain boundaries.

2.2. HALL EFFECT. — The Hall coefficient (R_H) of high T_c oxides shows unusual behaviour which has been studied by several groups. At very low doping levels R_H is T-independent with a magnitude corresponding to the number of added holes p as illustrated for $La_{2-x}Sr_xCuO_4$ [21] in Figures 5a and 5b. For $p > 0.05$ the Hall coefficient develops a marked T dependence. For $p > 0.1$ the magnitude of R_H becomes much smaller than the value expected from the number

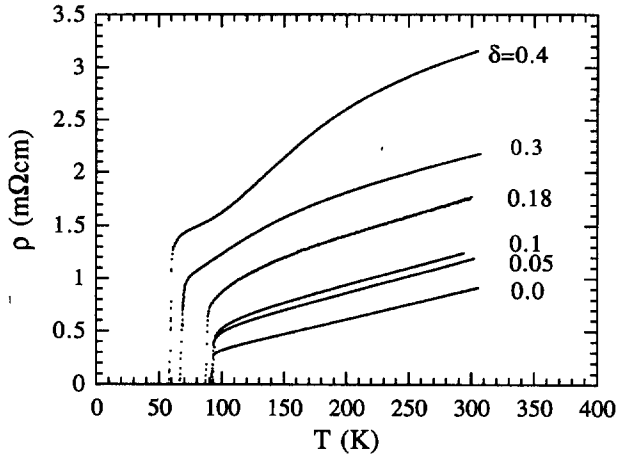

Fig. 4. — Resistivity of polycrystalline $YBa_2Cu_3O_{7-\delta}$ for the values of δ shown [11,20].

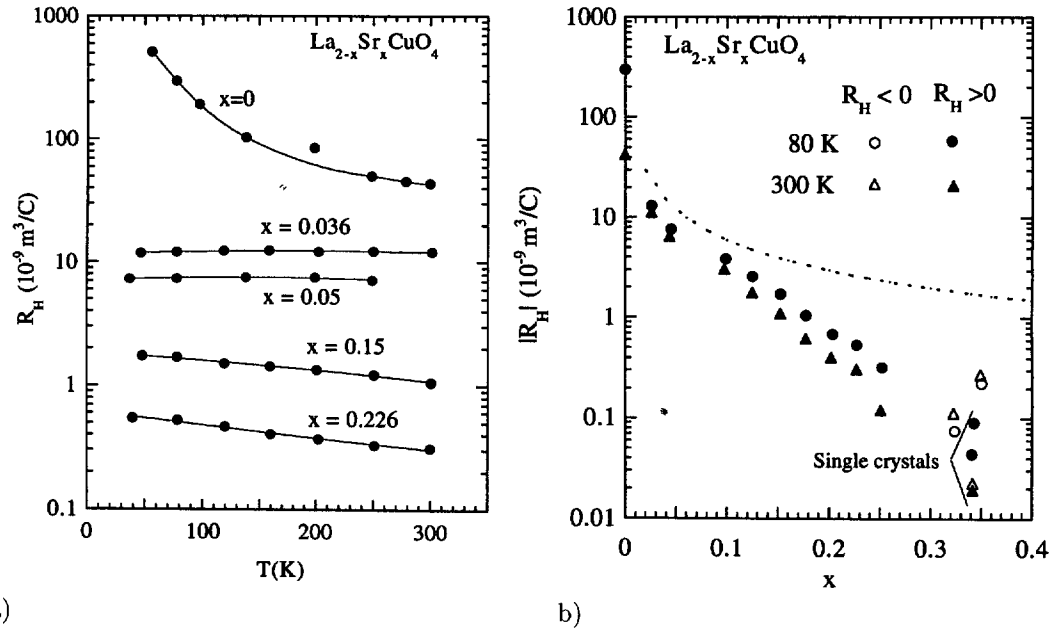

Fig. 5. — a) Temperature dependence of the Hall coefficient R_H for polycrystalline samples of $La_{2-x}Sr_xCuO_4$ [21]. b) $|R_H|$ *vs.* x at 300 and 80 K. Some single crystal data are also shown [21]. The dashed line corresponds to $R_H = V_f/ex$ where V_f is the volume per formula unit.

of added holes and R_H decreases exponentially with x (Fig. 5b) and for LSCO it changes sign for $p > 0.3$. The exponential dependence of R_H is found for other polycrystalline compounds as shown in early work on doped YBCO [22] and also in Figure 6a. The values of p used in Figure 6a for YBCO and the related $(Y_{1-x}Ca_x)Sr_2(Tl_{0.5}Pb_{0.5})Cu_2O_7$ compound [15,23] which has no CuO chains, have been derived from bond valence sum analyses [10,24], whereas those

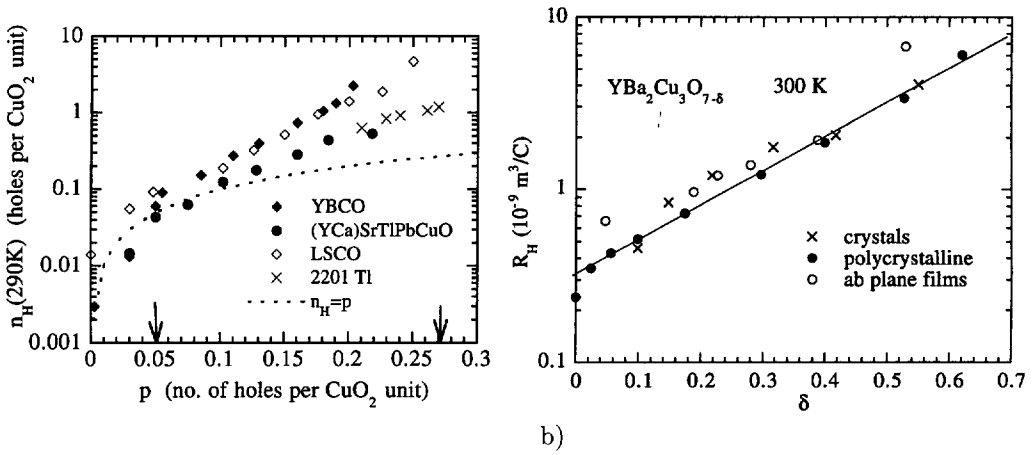

Fig. 6. — a) Analogous plots to Figure 5b for various polycrystalline samples – namely a logarithmic plot of the Hall number n_H at 290 K *versus* the number of added holes (p) per CuO_2 unit, with p estimated in various ways for different compounds (see text). The dashed line again corresponds to $n_H = p$. The vertical arrows mark the superconducting region. b) Comparison of room temperature Hall coefficient data for $YBa_2Cu_3O_{7-\delta}$ in the form of *ab* plane films, open circles [11], single crystals, crosses [15,27] and polycrystalline ceramics, closed circles [15,20].

for the single layer $Tl_2Ba_2CuO_{8+\delta}$ compound [25] have been derived from the values of T_c using the parabolic $T_c(p)$ relation [26]. The same procedure was also used to obtain the variation of the room temperature thermoelectric power (TEP) with p [24]. These results are indeed representative of the *ab* plane Hall coefficient of single crystals as illustrated by the comparison of Hall data for single crystal [27], thin film [11] and polycrystalline samples of YBCO [15,20] shown in Figure 6b.

The corresponding T dependence of R_H for *ab* plane YBCO films [11] is shown for various values of δ in Figure 7. There are substantial changes in the magnitude and T dependence of both R_H (Fig. 7) and ρ_{ab} (Fig. 3) as a function of δ. But as shown in Figure 8 the ratio of $\rho_{ab}/R_H(T) \equiv \rho_{xx}/\rho_{xy}$, σ_{xx}/σ_{xy} or $\cot(\Theta_H)$ the inverse Hall angle, varies much less with δ, by only about 20% while R_H and ρ_{ab} change by at least a factor 5 [11]. Similar data are obtained by other groups both for single crystals [27] and thin films [19,28,29] of $YBa_2Cu_3O_{7-\delta}$. It is often found that cot Θ_H obeys a T^2 power law. Indeed this observation in Zn doped $YBa_2Cu_3O_7$ crystals [30] was the key evidence in favour of the two lifetime model of Anderson [31] in which the conductivity is determined by the holon lifetime and the Hall angle by the spinon lifetime. In fact the data in Figure 8 show a gradual change in the exponent from T^2 to $T^{1.5}$ behaviour as δ is reduced from 0.28 to 0.05. Some curvature in cot Θ_H *vs.* T^2 is also observed for Ca doped YBCO films [32] (where optimum doping occurs with substantial oxygen deficiency in the Cu-O chains) so it does seem to be a property of the CuO_2 planes in YBCO. On the other hand cot Θ_H for $Bi_2Sr_2Ca_{1-x}Y_xCuO_8$ crystals [33] fits an $AT^2 + B$ law very well and again there is little change in A as T_c is reduced by underdoping. A similar situation is found for $Tl_2Ba_2CuO_{8+\delta}$ crystals [15] when T_c is reduced from 60 to 20 K by overdoping. In this case R_H is nearly T-independent on the overdoped side with a value corresponding to approximately 1 hole per CuO_2 unit as shown in Figure 9a. Its weak T dependence combined with the upward curvature in $\rho_{ab}(T)$ give a T^2 law for cot Θ_H (Fig. 9b).

To conclude this section we may say that the strong T-dependence of R_H is connected with the occurrence of superconductivity. Although both R_H and ρ_{ab} change strongly with hole

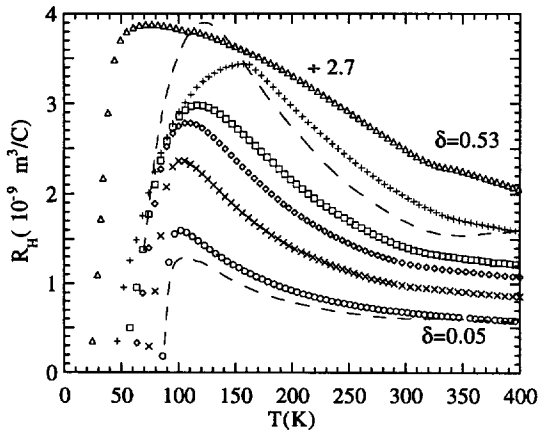

Fig. 7. — Temperature dependence of the Hall coefficient R_H for $YBa_2Cu_3O_{7-\delta}$ films with current in the ab plane and $H \parallel c$ axis [11]. Single crystal data shown by the dashed lines. The values of δ are the same as in Figure 3.

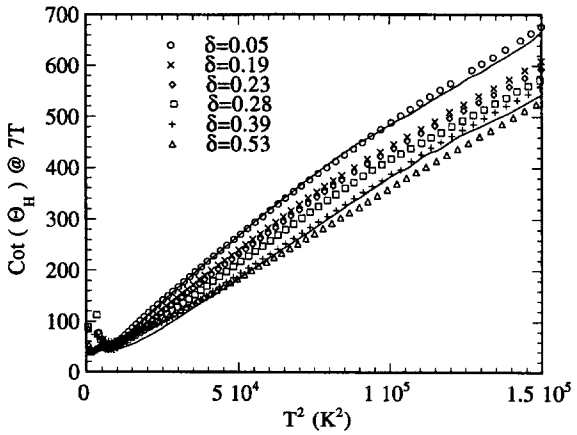

Fig. 8. — Plots of cot Θ_H ($\equiv \rho_{xx}/\rho_{xy}$) measured in a field 7 Teslas, *versus* T^2 for the same data as in Figures 3 and 7 [11].

concentration *and* show changes in slope associated with the opening of the normal state gap in the underdoped region, their ratio, the Hall angle, does not, and indeed shows similar behaviour for both underdoped and overdoped regions. We believe that the insensitivity of the Hall angle to doping level is a key result for understanding the normal state transport properties.

2.3. THERMOELECTRIC POWER. — The thermoelectric power or Seebeck coefficient of the hole doped cuprates varies strongly with doping and is usually positive. Typical behaviour for underdoped, optimally doped and overdoped compounds is shown in Figure 10 [24]. Unlike the resistivity the TEP is not sensitive to grain boundaries and measurements of polycrystalline samples invariably correspond to the ab plane thermopower of single crystals of the same

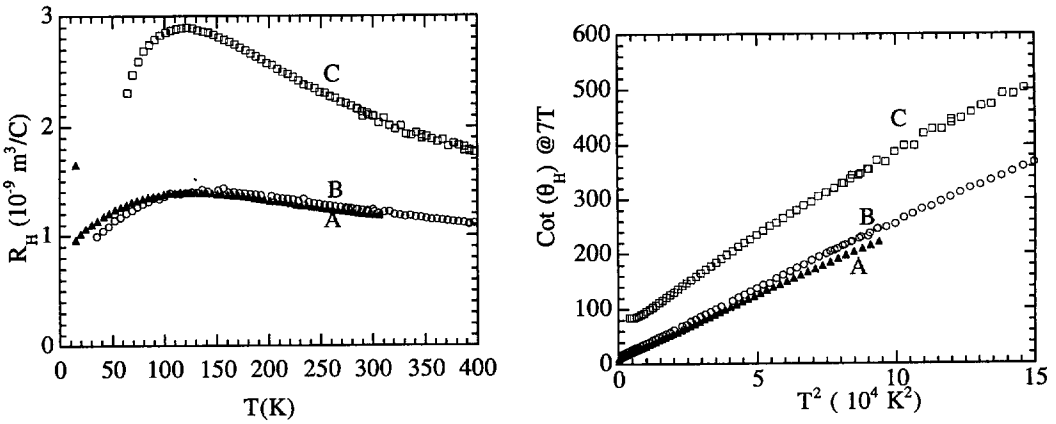

a) b)

Fig. 9. — a) Hall coefficient *vs.* temperature for three single crystals of $Tl_2Ba_2CuO_{6+\delta}$ with current in the *ab* plane and *H* along the *c* axis [15]. Crystals A, B and C have T_c values of 21, 28 and 62 K. b) Plots of cot Θ_H ($\equiv \rho_{xx}/\rho_{xy}$) measured in a field 7 Teslas for the same crystals [15].

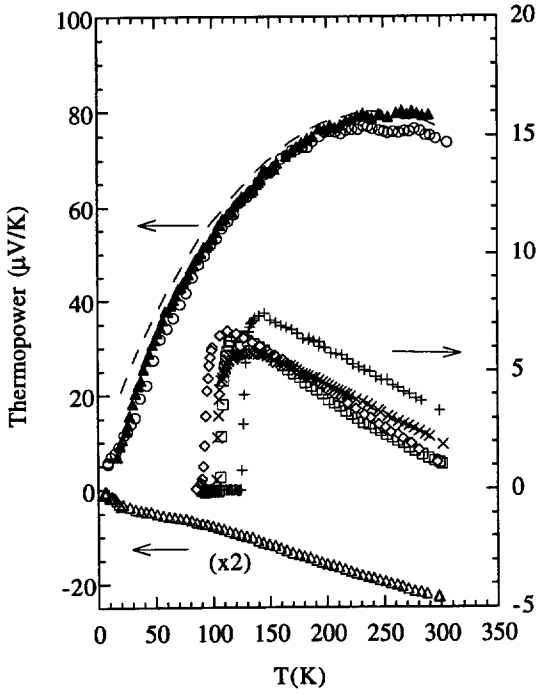

Fig. 10. — Representative behaviour [24] of the thermoelectric power for: a) underdoped samples: sintered $YBa_2Cu_3O_{6.36}$, open circles, $Y_{0.6}Ca_{0.4}Sr_2(Tl_{0.5}Pb_{0.5})Cu_2O_7$, closed triangles, and single crystal $Bi_2Sr_2(Y_{0.47}Ca_{0.53})Cu_2O_8$, dashed line (L.H. scale); b) optimally doped Bi 2212, open diamonds, $Y_{0.2}Ca_{0.8}Sr_2(Tl_{0.5}Pb_{0.5})Cu_2O_7$, crosses (x), Bi2223, squares-and Tl2223, crosses (+) (R.H. scale). c) Overdoped Tl2201, open triangles, (L.H. scale).

composition. This has been shown by direct comparison with data for single crystals in the literature, for example the underdoped Bi2212 crystal [34] in Figure 10 and by measurements on polycrystalline samples in which the grain boundaries were degraded in a controlled manner [35]. As the hole concentration is increased above the threshold value for superconductivity the broad maximum in the TEP shifts systematically to lower temperatures. For optimally doped compounds the maximum is presumably below T_c (since for a conductor the TEP $\rightarrow$ 0 as $T \rightarrow 0$) and the TEP follows a linear $\alpha T + \beta$ law with a finite intercept β of order $8 - 10$ μV/K (Fig. 10). However this is not invariably true, *e.g.* for the CuO_2 planes of YBCO (*i.e.* the a axis thermopower of untwinned crystals [36]) and for the single layer Tl2201 compound, $\beta = 0$ to 2 μV/K above 120 K with a marked increase below 100-120 K. On the other hand for optimally doped LSCO $\beta = 20$ μV/K at room temperature. Despite these differences, the room temperature TEP varies so systematically with p that it can be used as a guide to the hole concentration as shown in Figure 11 [24]. This is a somewhat surprising result, but the analysis of susceptibility and entropy described later does indicate that in high T_c cuprates the added holes occupy a narrow range of energies near the Fermi level [8, 37] (or more precisely induce spectral weight within about $+/-600$ K of the Fermi level) So it seems that the room temperature TEP is very sensitive to the spectral weight in this energy region.

An example of the use of TEP measurements for understanding the doping process is shown in Figure 12 [24,38] where the room temperature TEP of various $YBa_2(Cu_{1-x}M_x)_3O_{7-\delta}$ samples is plotted *versus* T_c. It can be seen that the points for all chain dopants, M = Ga, Cr, Co, and Al, lie on the same curve as O deficient YBCO, showing that the effect of these dopants is simply to reduce the planar hole concentration p. On the other hand Zn and Ni which substitute for the planar Cu(2) atoms clearly reduce T_c without substantially affecting p.

3. A Simple Model for the Transport Properties of High T_c Oxides

At the end of 1992 much of the experimental data described above was well documented. There was also evidence from angular resolved photo emission (ARPES) work for the existence of a large Fermi surface (FS) rather similar to that calculated [39] using band theory and the local density approximation. Neutron scattering [6, 7] and many NMR studies [40] already gave evidence for the importance of anti-ferromagnetic spin fluctuations with a well defined wave vector $\mathbf{Q} = (\pi/a, \pi/a)$ in the CuO_2 planes and a certain characteristic width, $\xi^{-1}(T)$ in $\mathbf{k}$ space which became much broader as p was increased. As sketched in Figure 13, [41], if the electrical resistivity were determined by electron-spin fluctuation scattering, then because all parts of the FS are not spanned by the characteristic wave vector $\mathbf{Q}(\pm\xi^{-1}(T))$ the mean free path would vary strongly around the FS. It was shown [41] how this picture gave a simple qualitative explanation of most of the above properties, including the large TEP (which is closely linked to the magnitude of ξ), the strong doping and T dependence of ρ_{ab} and R_H and the weaker doping dependence of cot Θ_H. Another supporting point was that $\rho_{ab}(T)$ and cot Θ_H of zinc doped samples had different T dependences and yet both approximately obeyed Matthiessen's rule. The latter rule is only expected to hold when the density of states or number of charge carriers, is T-independent and different scattering processes, *e.g.* potential scattering and in this case inelastic spin fluctuation scattering, are independent and additive. The viewpoint described above arose primarily from the nearly anti-ferromagnetic Fermi liquid picture (NAFL) of Pines and co-workers [42] who have now made detailed calculations of R_H and cot Θ_H [43]. It has also been discussed within the t-J model [44]. However since then a number of new experimental facts have emerged which are discussed in the following paragraphs. These new results show that the energy dependence of the excitation spectrum is of primary importance.

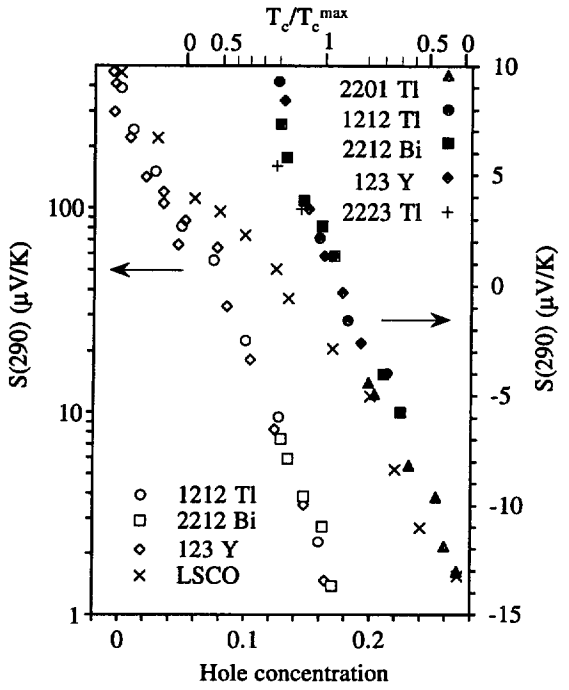

Fig. 11. — Room temperature thermoelectric power $S(290\ \mathrm{K})$ *versus* hole concentration (and T_c/T_c^{max}) for various underdoped (logarithmic L.H. scale) and optimally or overdoped compounds (linear R.H. scale). From reference [24] with additional data for $La_{2-x}Sr_xCuO_4$, crosses (x) (L.H. scale), which deviate from the universal curve for $x > 0.08$.

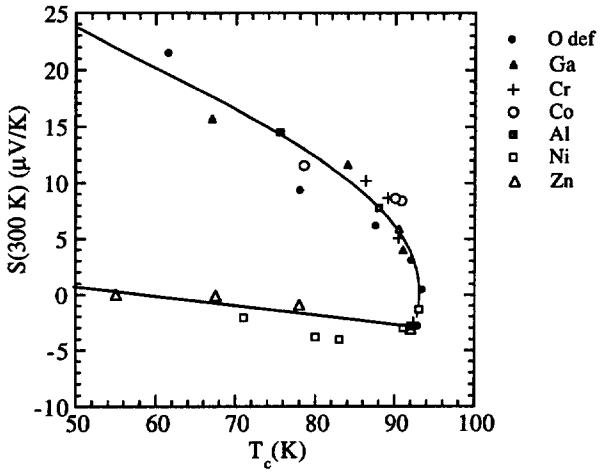

Fig. 12. — Room temperature thermoelectric power $S(300)$ *versus* T_c for various $YBa_2(Cu_{1-x}M_x)_3O_7$ compounds. The chain substituents M = Ga, closed triangles, Cr, crosses (+), Co, open circles and Al, closed squares, lie on the same curve as O deficient YBCO, closed circles. The data for plane substituents M = Zn, open triangles or Ni open squares [22], lie on another curve [24, 38].

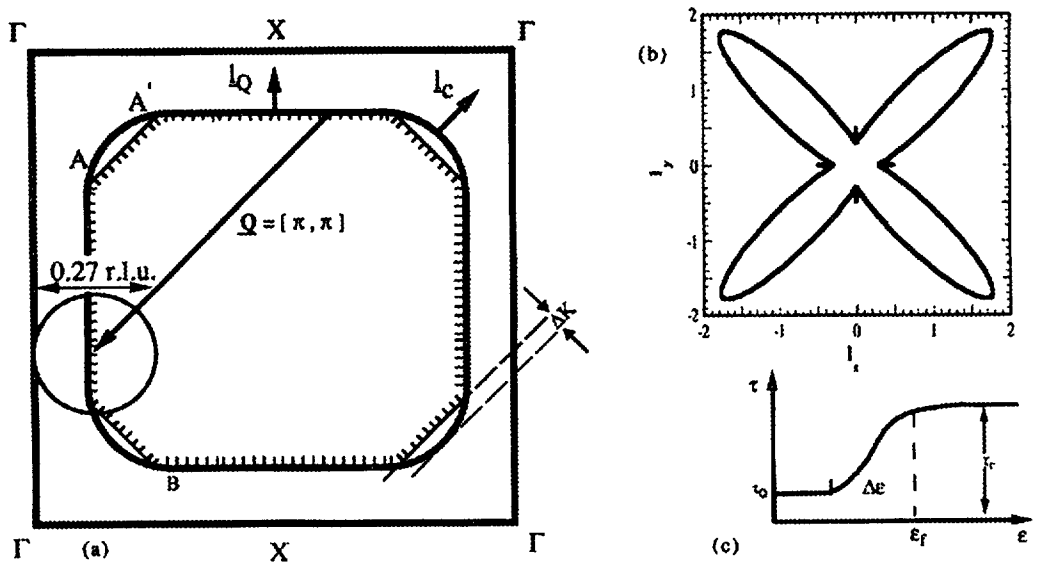

Fig. 13. — From reference [41]. a) Large Fermi surface similar to that calculated for the CuO_2 planes of $YBa_2Cu_3O_7$ using local density band theory [39]. The hatched regions are connected by the spin fluctuation **Q** vector but regions such as A-A′ are not. This gives rise to a strong variation in mean free path (l) around the FS illustrated in (b) as a plot of l_x *vs.* l_y. As shown in (c) there is also a strong energy dependence of the relaxation time in the regions A-A′ which is governed by the real space spin fluctuation correlation length $\xi(T)$ and which enhances the TEP. Note that the numerical value used for ξ^{-1} in this diagram is a factor of 1.4 larger than that measured for $YBa_2Cu_3O_{6.92}$ at 150 K by neutron scattering because of an error in reference [41]. (in the neutron scattering papers one r.l.u. refers to a reduced lattice unit, *i.e.* $\sqrt{2}\pi/a$ and not a reciprocal lattice unit).

4. Bulk Thermodynamic Properties

4.1. The Normal State Gap in YBCO. — The presence of a gap in the spin fluctuation spectrum of oxygen deficient (underdoped) YBCO has been established by neutron [6] and NMR studies [45–47] which show that the imaginary part of the spin susceptibility $\chi''(\mathbf{Q},\omega)$ develops a low frequency gap in the normal state above T_c. Below a certain temperature T^* there is also a decrease in the static spin susceptibility $\chi'(0,0)$ of underdoped samples and in the corresponding ^{89}Y [48] and ^{17}O NMR Knight shifts [45]. The precise relationship between the characteristic temperatures of the responses at $\mathbf{Q} = 0$ and $\mathbf{Q} = (\pi/a, \pi/a)$ is still being investigated and we will simply focus on the uniform ($\mathbf{Q} = 0$) response here. Initially the decrease in χ' was ascribed to a gap in the spin spectrum only, however specific heat studies [9] showed a drastic decrease in the height of the anomaly at T_c in underdoped YBCO (Fig. 14a). Integration of these data to give the electronic entropy S showed that S/T and the static susceptibility $\chi(T)$ had almost identical temperature dependences (Fig. 14b). Furthermore to within 20%, $S/\chi T$ is equal to the free electron Wilson ratio $a_0 \equiv \pi^2 k_B^2/3\mu_B^2$. The similar T dependences of S/T and χ show that the total spin/charge excitation spectrum (all **Q**) and the $\mathbf{Q} = 0$ spin excitation spectrum have similar energy dependences. This would not preclude the possibility that the normal state gap exists in the spin spectrum alone if the normal state entropy were dominated by spin excitations. However we believe that this is excluded by the proximity of the Wilson ratio to its free electron value. This result does not require that the

respective spectra are those of free electrons but rather that the relative number of thermally excited charge and spin excitations is that expected for conventional fermions. Thermally excited fermions contribute $k_B \ln(4)$ to the entropy (with equal contributions from charge and spin), and $\mu_B^2/2$ to $k_B \chi T$ (Ref. [37]), values which account for both the Wilson ratio of free electrons and the ratio $S/\chi T$ in the normal state and pseudogap regions of $YBCO_{7-\delta}$ and [37] and LSCO [8]. If the spectrum were dominated by spin excitations then the Wilson ratio would be a factor of two smaller than observed. We conclude from this thermodynamic data that charge and spin excitations make comparable contributions to the normal state entropy and that the normal state gap is present in both charge and spin excitations.

This fact places constraints on possible theoretical descriptions of the normal state but it does not necessarily mean that electron-electron correlations are unimportant. For example the heavy fermion superconducting compound $CeCu_2Si_2$, which has a mass enhancement of 1000 and a superconducting transition temperature of 0.6 K, also has a Wilson ratio close to the free electron value [49]. However the close numerical correspondence between S and χT shown in Figure 14b suggests that an analysis in terms of an energy (E) dependent fermion density of states, $g(E)$ may be appropriate. This would be the case if the normal state gap resulted from

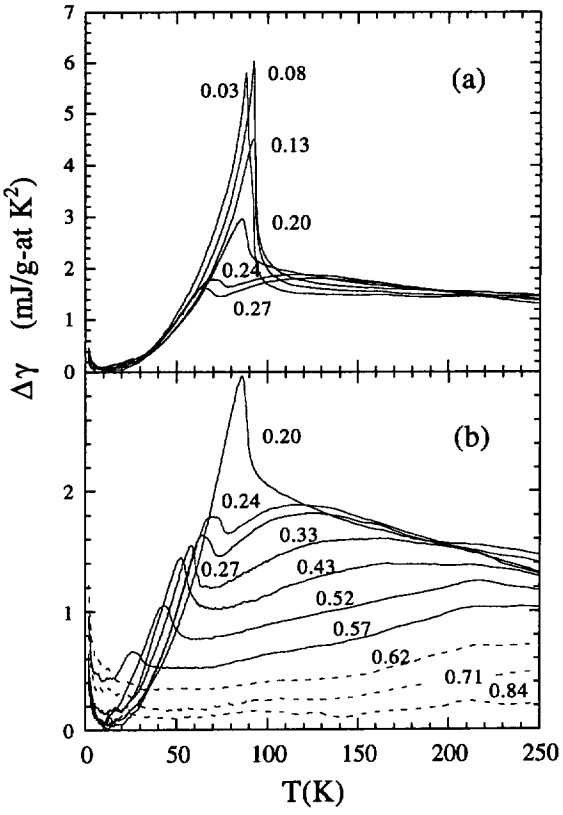

a)

Fig. 14. — a) Electronic specific heat coefficient of various $YBa_2Cu_3O_{7-\delta}$ samples relative to $YBa_2Cu_3O_6$ [9] for the values of δ shown. b) From reference [37], upper part, $\Delta S/T$ *versus* T for the samples in Figure 14a, where ΔS is the electronic entropy. Lower part, static susceptibility data for similar samples. a_0 is the free electron value of the Wilson ratio (see text).

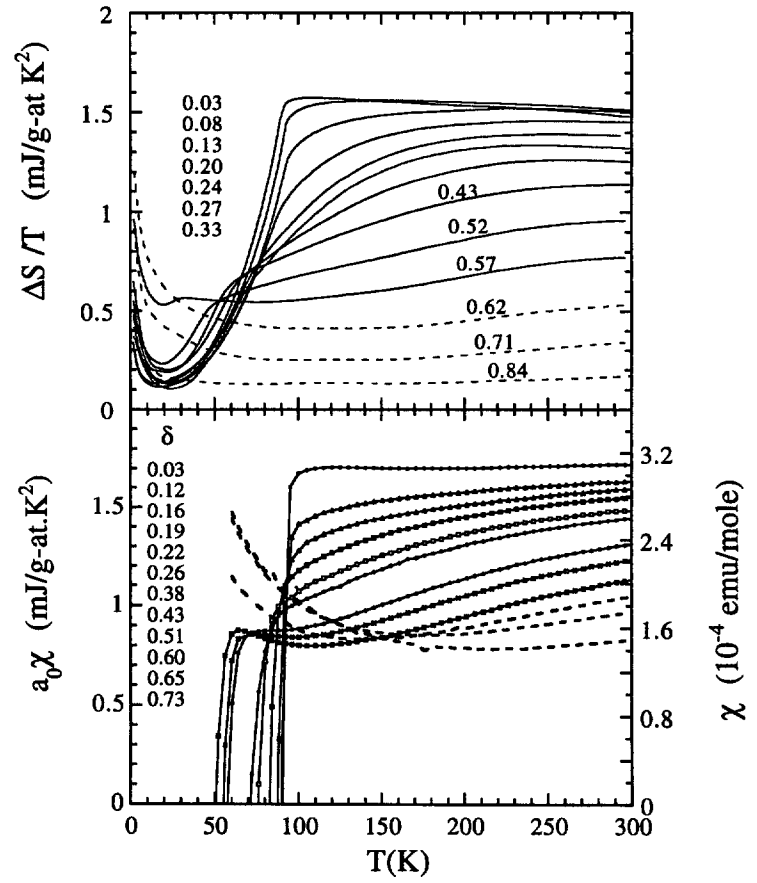

Fig. 14. — *(Continued.)*

precursor pairing or a density wave instability. However for simplicity it has been assumed that $g(E)$ is not temperature dependent. From a standard analysis using Fermi statistics it turns out that in this model the T dependence of the electronic specific heat coefficient γ and the quantity $\chi^*(T) \equiv \mathrm{d}(\chi T)/\mathrm{d}T$ closely follow the E dependence of $g(E)$ [37] near the Fermi energy E_F. In more general cases $\gamma(T)$ and $\chi^*(T)$ reflect the energy dependences of the total and spin excitation spectra respectively.

Figure 15 shows fits of $\chi^*(T)$ to a "d-wave" form of $g(E)$ that is symmetric about E_F and which goes linearly to zero as $E \to E_\mathrm{F}$, but with a states conserving peak at an energy Δ similar to the quasiparticle DOS of a d-wave superconductor. It can be seen that the "d-wave" normal state form of $g(E)$ gives a slightly better fit to the χ^* data than a non-states conserving triangular gap. Furthermore all χ^* curves extrapolate linearly to the same point at $T = 0$, which corresponds to the zero of the spin susceptibility as determined by NMR [37, 40]. In making these fits the free parameters are the normal state gap Δ and the spin susceptibility χ_0 at very high temperatures. These are plotted *versus* oxygen content δ in Figure 16. It is interesting to note that for $\delta > 0.7$, the gap Δ approaches a value which is quite close to the accepted value of the antiferromagnetic exchange interaction J between nearest neighbour Cu spins. The normal state gap $\Delta \to 0$ for optimally doped compositions. The parameter χ_0 is

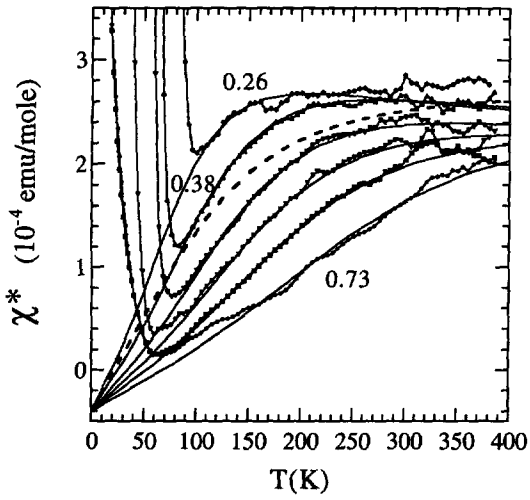

Fig. 15. — $\chi^*(\equiv d\{\chi T\}/dT)$ data for the samples in Figure 14b for δ values of 0.26, 0.38, 0.51, 0.60, 0.65 and 0.73. The solid lines show fits for a d-wave normal state gap with free parameters Δ and χ_0 (see text), the dashed line shows the best fit obtained for a triangular gap for $\delta = 0.38$ [37].

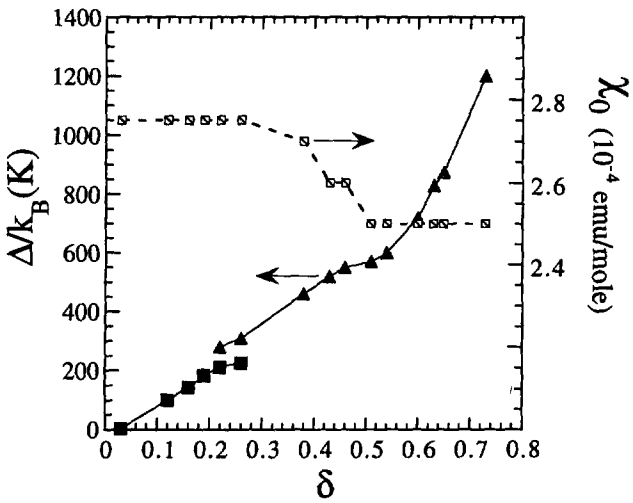

Fig. 16. — Values of the normal state gap parameter Δ (solid triangles and solid squares) and the background Pauli paramagnetism χ_0 (open squares) corresponding to the normal state d-wave gap in $YBa_2Cu_3O_{7-\delta}$ are plotted *versus* oxygen deficiency δ (from Ref. [37]).

constant for oxygen deficiencies from $\delta = 0$ to 0.3 (the region of the first plateau in T_c *vs.* δ) and then falls smoothly by 10% to another constant value at $\delta = 0.5$ (the end of the 60 K plateau).

4.2. THE NORMAL STATE GAP IN LSCO. — Similar measurements and analysis have recently been completed for $La_{2-x}Sr_xCuO_4$ [8] over a wide doping range $0 < x < 0.45$, going from the

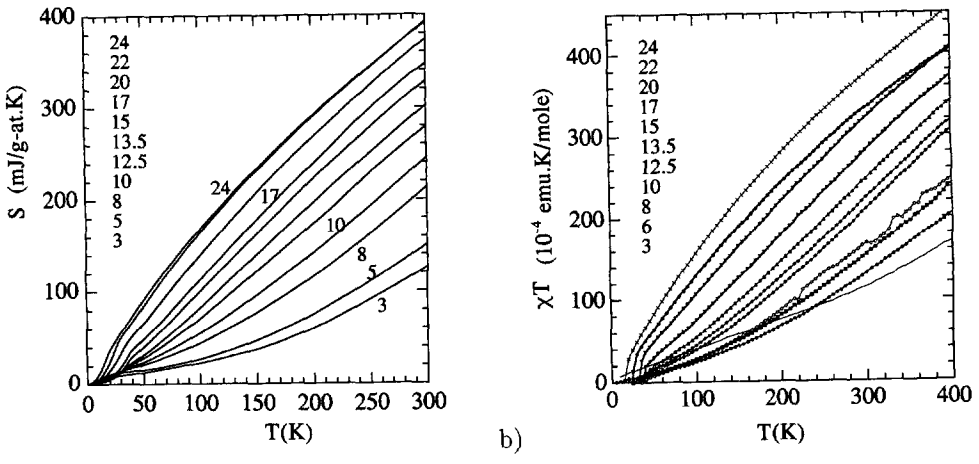

Fig. 17. — a) Electronic entropy S *versus* temperature for various $La_{2-x}Sr_xCuO_4$ samples [8]. x values are given in %. b) Corresponding measurements of the susceptibility χT for the same samples [8].

antiferromagnetic, insulating to the strongly overdoped state. The $\chi(T)$ data are in good agreement with previous work, and the comparison of χT and S is shown in Figures 17a and b. For LSCO the magnitude of the spin susceptibility (*i.e.* the contribution to the total susceptibility from Van Vleck and Landau terms) is not known as precisely as for YBCO. Using the measured values of the total susceptibility gives a Wilson ratio $\chi T/S$ which is very close to a_0 the free electron value as found for YBCO. Changes in χ with doping are independent of the zero in spin susceptibility and over a wide range of x, plots of χ *vs.* S/T at fixed T give a slope equal to a_0 to within 20% . The same analysis has therefore been made to obtain the excitation spectrum on the assumption that the T-dependences of γ and χ^* arise from an energy dependent single particle density of states $g(E)$.

As shown in Figure 18 for $x < 0.17$, $g(E)$ again shows a linear dependence at low energies and can again be fitted reasonably well by the states conserving d-wave form of $g(E)$ used for YBCO. However in the region $0.17 \leq x \leq 0.22$ there is only a small linear region which appears to extrapolate to a finite DOS at E_F. For larger values of x there is simply a peak in $g(E)$ at E_F which gradually becomes smeared out as x is increased into the heavily overdoped region. It is possible that this behaviour is a general feature of overdoped cuprates but this obviously needs to be verified for other compounds such as Ca doped YBCO.

At the present time there seems to be several possible ways of accounting for the d-wave like normal state gap. One possibility is that it is caused by precursor superconducting pairing of carriers well above the superconducting transition temperature as in the picture suggested by Emery and Kivelson [50]. Here Cooper pairs are formed at high temperatures but the carrier density is so low that the phase coherence responsible for bulk superconductivity only sets in at much lower temperatures.

A second possibility is that it is a magnetic effect. Several NMR groups have suggested that there is a localised magnetic moment on the planar Cu atoms, at least for under- and optimally-doped compositions. For LSCO this is most clearly shown by the measurements of ^{63}Cu $1/T_1$ at high temperatures [51]. These basically show the same behaviour for compositions between $x = 0$ and $x = 0.15$. Furthermore the anti-ferromagnetic exchange interaction between nearest neighbour Cu spins $J = 0.13$ eV is almost independent of x. In any picture where the doped holes coexist and interact with localised Cu spins it is quite plausible that their

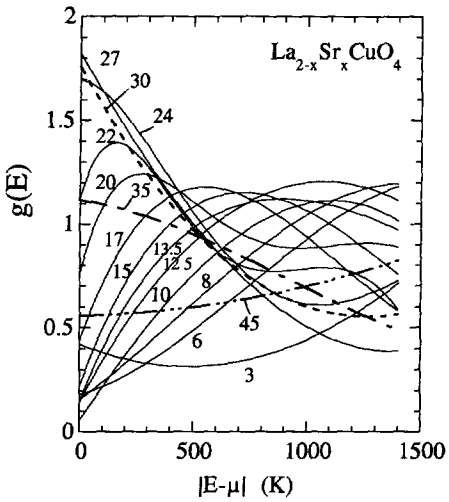

Fig. 18. — Energy dependent density of states derived from susceptibility data such as those in Figure 17b using the procedure described in reference [37].

mutual interaction would depend on the direction in which the holes are moving. Specifically there would be weak or even zero interaction for holes propagating at 45° to the Cu-O bonds because for well-ordered spins there is no alternation of spin orientation in those directions. Thus for those directions there could be zeros in the magnetically induced gap, mimicking the $d_{x^2-y^2}$ symmetry of the superconducting gap. We should also mention that several theoretical treatments of Anderson's resonating valence bond (RVB) picture [52, 53] imply that the spin excitation gap has d-wave symmetry above the superconducting critical temperature.

A third possibility is the so-called "soft Coulomb gap" induced by strong electron-electron interactions especially in a 2D electron gas. This has been seen in other materials [54] but there it generally arises from a combination of electron-electron scattering and disorder.

Recent experiments [55] in which the superconductivity of LSCO is suppressed by magnetic fields as high as 60 T show that for $x < 0.15$ the ground state is not metallic in that both the in-plane (ρ_{ab}) and out-of-plane (ρ_c) resistivities increase as $\ln T$ down to the lowest temperatures studied. On the other hand for $x > 0.15$ a metallic ground state in which ρ_{ab} and ρ_c are constant as $T \to 0$ is obtained when superconductivity is suppressed by high magnetic fields. This point is consistent with the form of $g(E)$ shown in Figure 18. However in the absence of detailed theoretical predictions, the high field experiments do not really distinguish between the possibilities mentioned above. Namely precursor pairs with an energy gap ≈ 500 K would probably not be suppressed by fields of 60 Tesla for which the Zeeman energy $\mu_B H/k_B = 40$ K. Nor would such fields suppress magnetic interactions, because the interaction energy, $J \approx 1600$ K, is also much larger than the Zeeman energy.

5. Effects of Zn Doping

5.1. Superconducting Properties. — Although Zn atoms certainly have a full d^{10} shell in the solid state, substitution of Zn for Cu in $YBa_2(Cu_{1-y}Zn_y)_3O_7$ gives the largest depression of T_c for any known dopant. As shown in Figure 19, Zn has an even stronger effect for underdoped (oxygen deficient) compositions. From measurements of specific heat [56], NMR [57] and Gd^{3+}

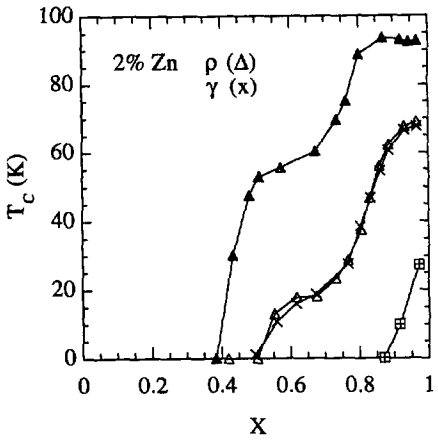

Fig. 19. — T_c values for various $YBa_2(Cu_{1-y}Zn_y)_3O_{6+x}$ samples *versus* oxygen content x, as determined from the peaks in the derivative of C_V/T (solid triangles $y = 0$, crosses $y = 0.02$ and squares $y = 0.07$) or of the resistivity (2% Zn sample open triangles).

ESR [58] for $YBa_2(Cu_{1-y}Zn_y)_3O_7$ it is clear that Zn doping gives rise to unpaired electrons in the superconducting state, namely there is a large residual density of states below T_c. For a d-wave superconductor any elastic scattering centre is expected to suppress T_c and increase the residual DOS simply because it mixes states with positive and negative values of the order parameter. However at present, and in the absence of detailed calculations using the known scattering cross section of the Zn atoms [59, 60] other possible mechanisms should also be considered. For example, if the Cu d spins are actually necessary for superconductivity then their replacement by non-magnetic Zn could suppress superconductivity locally [56] (*e.g.* within a superconducting coherence length of the Zn atom), and give rise to the residual density of states mentioned above. More precisely, as discussed below, Zn substitution seems to cause a shift in quasi-particle spectral weight (density of states) from higher to lower energies. If these lower energy states are non-propagating (localised) quasi-particle states then they will not contribute to the superconducting condensation energy and T_c will fall. This latter viewpoint is more consistent with our analysis of the normal state properties and raises the intriguing concept that the Cu d spins are actually necessary in order for the doped holes to propagate in the cuprates.

5.2. MAGNETIC SUSCEPTIBILITY ABOVE T_c. — Experimentally it is clear that for $YBa_2Cu_3O_7$ [59] and especially $La_{2-x}Sr_xCuO_4$ [61–63] and oxygen deficient YBCO [63], Zn substitution does give rise to an upturn in $\chi(T)$ at low temperatures. Some of our own data for $YBa_2Cu_3O_7$ doped with Zn [63], Co [64] or Ni [65] are shown in Figure 20a. Above 200 K the effect of Zn is much smaller than that of the other two elements which have well defined magnetic moments of 1.7 and $3.9\mu_B$ per Ni or Co atom respectively. For Ni and Co the temperature independent magnetic moment adds a constant to χT which therefore increases linearly with T. On the other hand for Zn doping χT is curved below 200 K (Fig. 20b). This latter behaviour has been attributed to Zn causing magnetic moments on neighbouring Cu atoms with ferromagnetic interactions and hence a Curie-Weiss law $\chi = C/(T - \theta)$ [59]. NMR measurements of an ^{89}Y satellite line support the presence of a Zn moment [66] although the satellite splitting follows a Curie rather than Curie-Weiss behaviour. On the other hand Gd^{3+} ESR studies [68] suggest

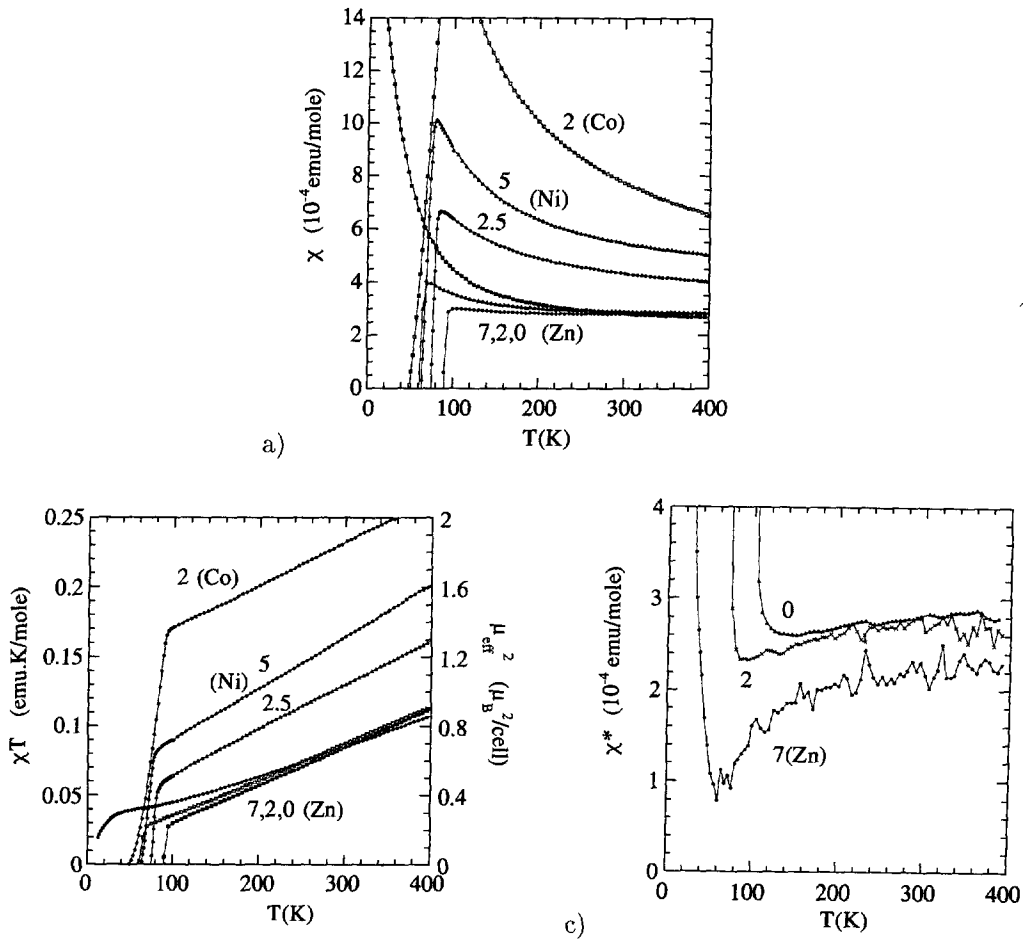

Fig. 20. — Plots of a) χ and b) χT for various $YBa_2(Cu_{1-x}M_x)_3O_7$ compounds, M = Co, Ni or Zn with x values in %; c) plots of the derivative χ^* ($\equiv d\{\chi T\}/dT$) for the Zn samples, showing a shift in spectral weight from higher to lower energies, leading to a gap in the spin spectrum for 7% Zn in $YBa_2Cu_3O_7$.

that Zn doping does not give rise to a magnetic moment on the CuO_2 planes although it may cause a moment on the CuO chains. Also we note that because any moment induced by Zn doping is certainly small (~ 0.4 to $0.6\mu_B$ per Zn atom) it is much more difficult to prove that the Curie-Weiss term increases linearly with Zn concentration and rule out effects caused by nearest neighbour pairs of Zn atoms.

An alternative picture is to say that Zn doping modifies the excitation spectrum and shifts spectral weight from high to low energies. From this viewpoint the χ^* plots for the 7% Zn doped sample in Figure 20c show that the curvature in χT is partly the result of extra states near $E = 0$, which give an upturn in χ^* at low temperatures and partly the result of a gap-like feature resulting from the redistribution of spectral weight from higher to lower energies. (For samples which are still superconducting in the measuring field of 5 T *e.g.* the 0 and 2% Zn samples in Figure 20c, there is an additional upturn in χ^* from the diamagnetism). This sort of picture also gives a consistent description of the effects of Zn doping on the susceptibility

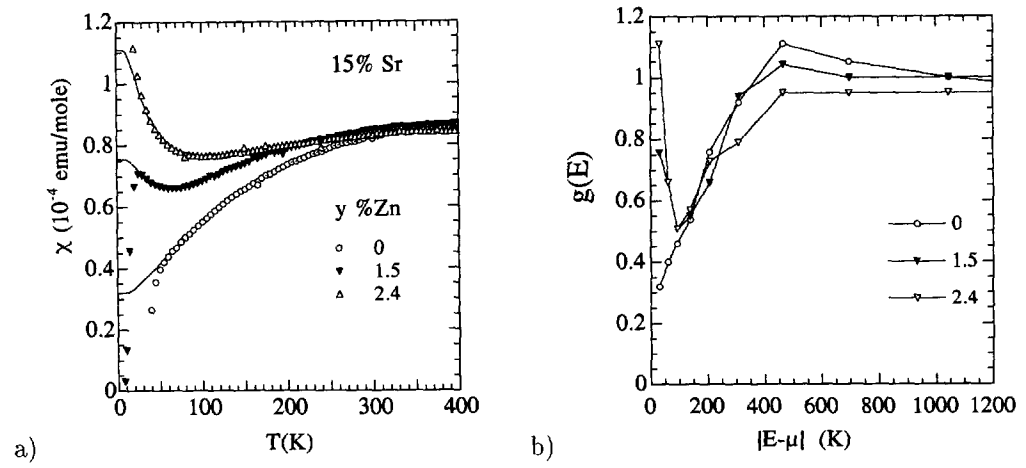

Fig. 21. — a) Measured values of susceptibility *versus* temperature for various $La_{1.85}Sr_{0.15}Cu_{1-y}Zn_yO_4$ ceramics. The solid line shows curves generated using the energy dependent DOS $g(E)$ given in (b). Zn doping smears out the peak in $g(E)$ near 400 K and introduces extra states near $E = 0$.

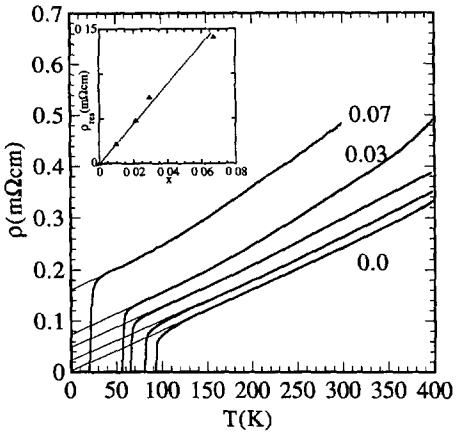

Fig. 22. — *ab* plane resistivity of laser ablated $YBa_2(Cu_{1-x}Zn_x)_3O_7$ films [68] with $x = 0, 0.01$, 0.02, 0.03 and 0.07. Insert shows that the extra temperature independent resistivity increases linearly with x.

of LSCO (Fig. 21) and of our unpublished susceptibility data for oxygen deficient, Zn-doped YBCO.

5.3. RESISTIVITY. — The effects of Zn doping on the resistivity of $YBa_2Cu_3O_{7-\delta}$ and $La_{2-x}Sr_xCuO_4$ are reasonably well established; studies have been made on polycrystalline [59, 67], epitaxial thin film [68] and single crystal samples [12] and the scattering cross section has been calculated using a phase shift analysis [60]. At optimum hole concentration Zn doping causes the parallel shift of $\rho_{ab}(T)$ curves shown in Figure 22 [68] corresponding to Matthiessen's rule. The extra T-independent resistivity increases linearly with Zn concentration as expected for so-called "single impurity" scattering. However, at higher Zn concentrations ($y > 0.03$)

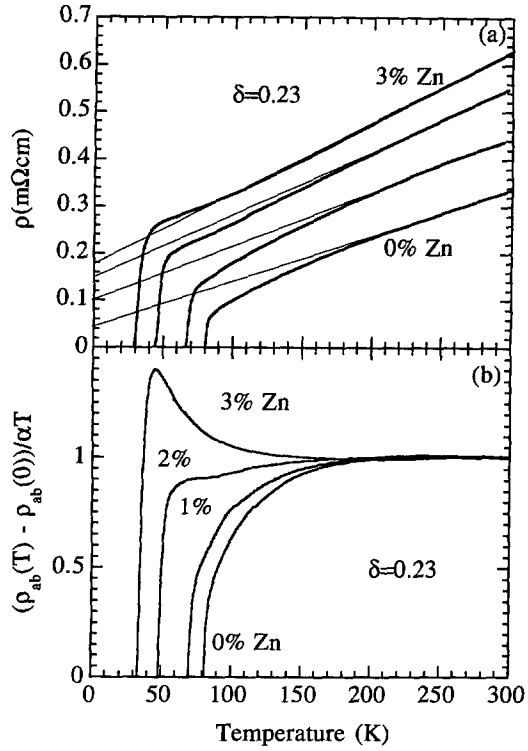

Fig. 23. — a) Effect of Zn doping on $YBa_2(Cu_{1-x}Zn_x)_3O_{6.77}$ films with $x = 0$, 0.01, 0.02 and 0.03 [68]. The downward curvature associated with the normal state gap is reduced, but as shown more clearly in b) the onset temperature remains near 180 K [68].

there is a tendency for $\rho(T)$ of $YBa_2(Cu_{1-y}Zn_y)_3O_{6.95}$ to show a slight upward curvature with larger values of $d\rho/dT$ near 300 K [59, 68]. This behaviour is also apparent in single crystal studies [12, 30].

As shown in Figure 23a the downward curvature in $\rho(T)$ associated with the normal state gap in oxygen deficient $YBa_2Cu_3O_{7-\delta}$ is reduced by Zn doping (especially for $y > 0.02$). However, as far as we can tell, the onset temperature, which is a measure of the normal state gap, is not altered (Fig. 23b). We should also note that the absence of downward curvature in the resistivity for $y > 0.02$ does not necessarily imply that the normal state gap is destroyed, since incipient localisation of low energy states would contribute a semiconducting T-dependence to the resistivity

5.4. HALL EFFECT. — The *ab* plane Hall effect of $YBa_2Cu_3O_7$ is altered in a rather complicated way by Zn substitution [30] and the simpler dependence, $\cot\Theta_H = AT^2 + B$, [30] with A constant and B proportional to Zn content, was strong evidence in favour of the two-lifetime model of Anderson [31]. Our results for epitaxial thin films [69] of $YBa_2(Cu_{1-y}Zn_y)_3O_7$ shown in Figure 24 are in broad agreement with those of reference [30]. One important difference is that in our work the high temperature value of R_H is more independent of Zn doping, *i.e.* Zn seems to have a larger effect at low temperatures — as found for χT (Fig. 20b) and for the thermoelectric power discussed in the following section. Despite this difference, as shown

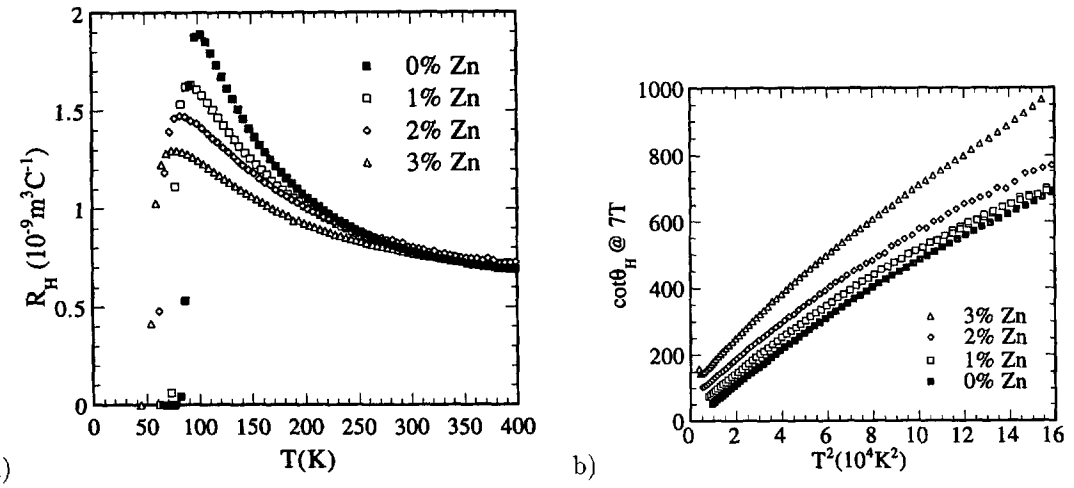

Fig. 24. — a) Hall coefficient of *ab* plane $YBa_2(Cu_{1-x}Zn_x)_3O_7$ films [69] and b) corresponding plots of cot Θ_H ($\equiv \rho_{xx}/\rho_{xy}$) measured at 7 T *versus* T^2 (Ref. [70])

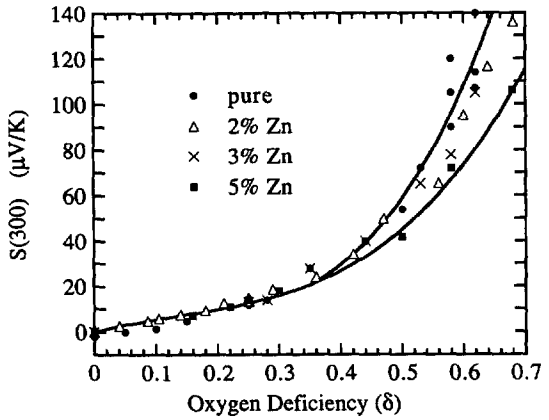

Fig. 25. — Room temperature thermoelectric power $S(300)$ *versus* oxygen deficiency δ for various $YBa_2(Cu_{1-x}Zn_x)_3O_{7-\delta}$ samples [72].

in Figure 24, cot Θ_H for our Zn doped samples also approximately follows at T^2 law with a temperature independent residual scattering rate. This effect of Zn is in contrast to the effects of hole doping (*e.g.* induced by oxygen deficiency [11] or Co doping [70]) where there is a slight reduction in slope but little change in the residual scattering term. The fact that cot Θ_H is not sensitive to the growth of the normal state gap with underdoping remains a challenge to theorists.

5.5. THERMOELECTRIC POWER. — The effect of Zn doping [72] on the room temperature TEP of $YBa_2Cu_3O_{7-\delta}$ is shown in Figure 25. Surprisingly, although Zn is a strong scatterer, *e.g.* 5% Zn increases $\rho_{ab}(300)$ by 50%, the room temperature TEP is much more sensitive to hole concentration (*i.e.* in this case oxygen deficiency δ) than to Zn content. However, there is a small effect which is more apparent in the T-dependent results shown in Figure 26. Namely

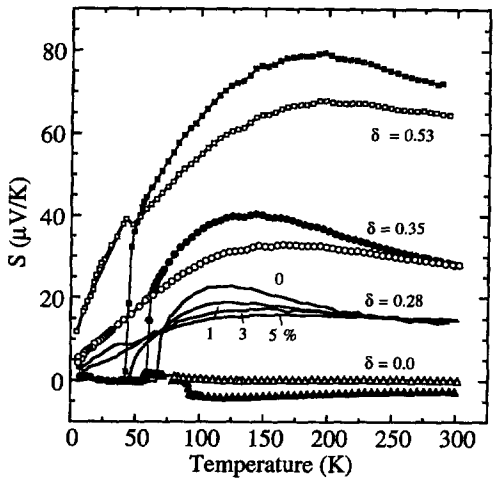

Fig. 26. — Temperature dependent thermoelectric power for several $YBa_2(Cu_{1-x}Zn_x)_3O_{7-\delta}$ samples. Closed symbols $x = 0$, open symbols $x = 0.03$ [72].

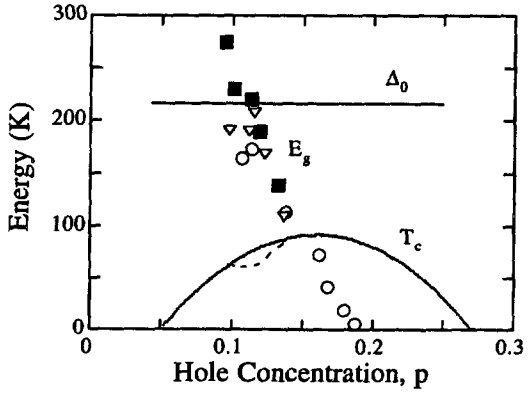

Fig. 27. — Normal state energy gaps deduced in various ways for $YBa_2Cu_3O_{7-\delta}$ plotted *versus* p the number of added holes/CuO_2 unit [72]. Solid squares, from the effect of Zn on the TEP, circles from specific heat, triangles from NMR Knight shift data.

the Zn-doped and Zn-free TEP results start to deviate below a certain temperature and this provides another way of estimating the normal state gap [72]. Similar behaviour over a wider range of hole doping has been found for Zn doped $(Y, Ca)(Ba, La)_2[Cu_{1-y}Zn_y]_4O_8$ [72]. The TEP results for $YBa_2(Cu_{1-y}Zn_y)_3O_{7-\delta}$ combined with specific heat and NMR Knight shift data, give a consistent picture for the hole dependence of the normal state gap as sketched in Figure 27. From this figure it appears that the gap goes to zero at optimum doping. In some ways the gap appears to be necessary for the occurrence of superconductivity. If it is too large then not enough entropy is available for superconductivity — but if it is too small then T_c falls again. However even though the gap is zero on the overdoped side there is still a small but finite energy scale as originally shown by analysis of Hall data for overdoped $La_{2-x}Sr_xCuO_4$ [73]. The results for $g(E)$ in Figure 18 show that there is no inconsistency here, although there is

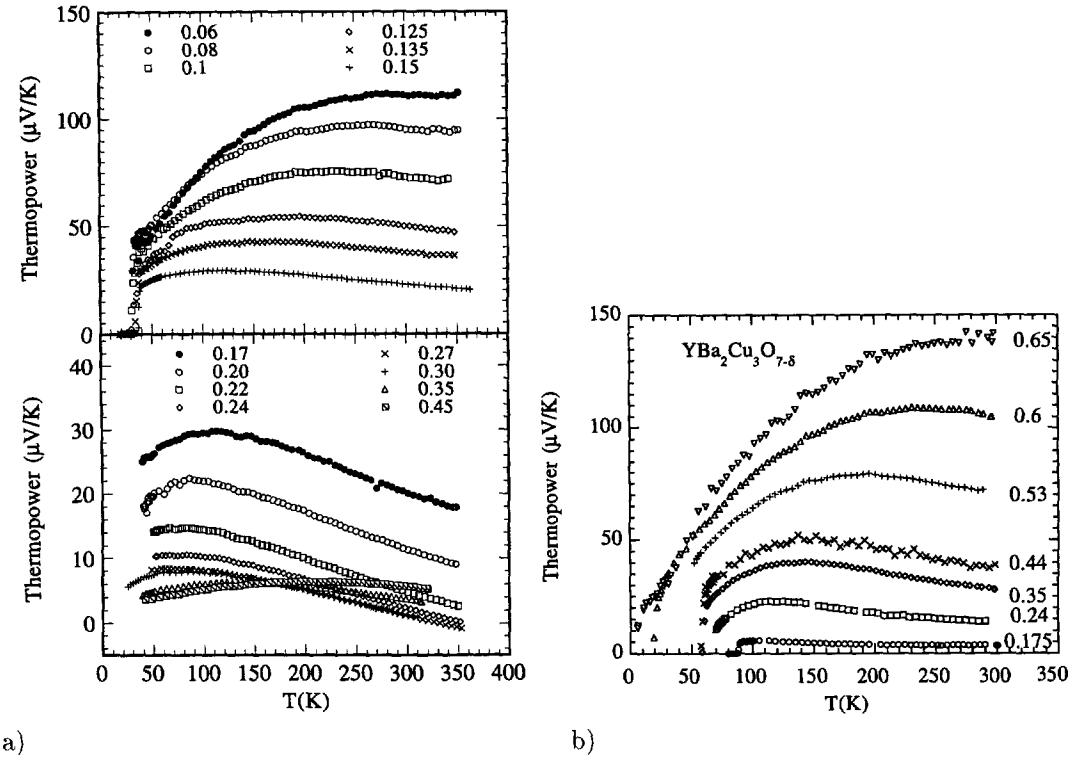

Fig. 28. — a) Thermoelectric power data for the same $La_{2-x}Sr_xCuO_4$ samples as in Figure 17. b) Some recent thermoelectric power data for $YBa_2Cu_3O_{7-\delta}$ including data from reference [72].

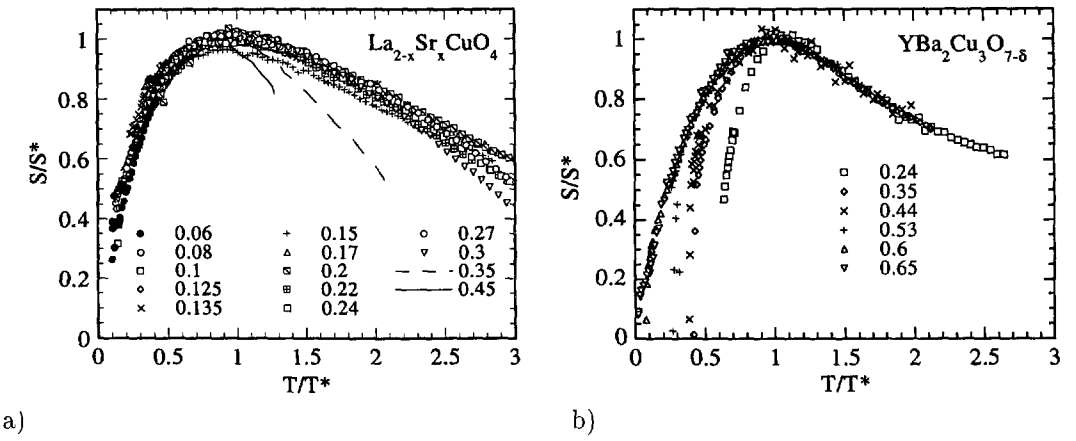

Fig. 29. — Scaling plots for thermoelectric power data in Figure 28. S/S^* *versus* T/T^* for: a) $La_{2-x}Sr_xCuO_4$; b) $YBa_2Cu_3O_{7-\delta}$.

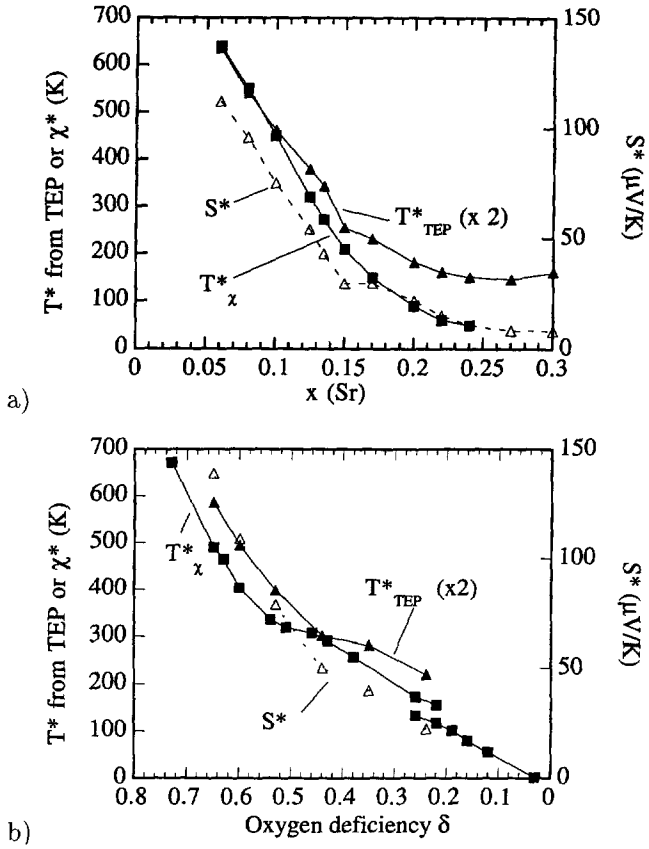

Fig. 30. — Parameters used for thermopower scaling. a) For $La_{2-x}Sr_xCuO_4$ L.H. scale: closed triangles, T^* values from TEP (×2), and squares from maxima (at $T = T^*_\chi$) in $\chi^*(T)$. R.H. scale: open triangles, S^* values used for TEP scaling. b) For $YBa_2Cu_3O_{7-\delta}$ L.H. scale: closed triangles, T^* values from TEP (×2), and squares from fits of χ^* to d-wave formula using the relation [37] $T^*_\chi = 0.56\Delta$ and the values of Δ in Figure 16. R.H. scale: open triangles, S^* values used for TEP scaling.

no gap on the overdoped side, there is still an energy-dependent enhancement of $g(E)$, whose width defines a small characteristic energy.

6. Scaling of the Thermoelectric Power

The analysis of the specific heat and magnetic susceptibility described above encouraged us to treat the thermoelectric power in a similar way. Typical data measured for $La_{2-x}Sr_xCuO_4$ and $YBa_2Cu_3O_{7-\delta}$ are shown in Figures 28a and b. When there is a well defined peak in the TEP, the scaling factors are easily found as the TEP value (S^*) and temperature (T^*) of the peak. If not, then suitable values of the scaling factors can usually be found from log-log plots. As shown in Figure 29a, for LSCO there is good scaling from $0.1 < T/T^* < 2.5$, for x values spanning the whole of the range where a superconducting ground state is observed ($0.06 < x < 0.30$). For $YBa_2Cu_3O_{7-\delta}$ there is also good scaling over similar range of T/T^* for a wide range of δ values although the peak in S/S^* is somewhat more pronounced than for LSCO. As shown in Figure 30, for both LSCO and YBCO the values of $2T^*$ needed to give this

scaling are in good agreement with the temperatures T^*_χ of the maxima in χ^* (for a d-wave gap $T^*_\chi = 0.56\ \Delta$ [37] where Δ is the normal state gap shown for YBCO in Fig. 16). However the values of S^* do change drastically with hole content (unlike the parameter χ_0 in Fig. 16 or the ratio S^*/T^*). This implies that S/T might well be a more fundamental scaling variable, although of course it must also give equally good scaled plots as those in Figure 29 but with a different functional form.

7. Conclusions

It seems that there are many unusual but systematic patterns in the normal state bulk properties of high T_c cuprates which are gradually being elucidated. The thermodynamic properties S (entropy) and χT can be understood in terms of a single energy-dependent excitation spectrum. The latter can be modelled by an energy-dependent fermion density of states $g(E)$ which has a gap with line nodes on the underdoped side of the T_c-hole concentration diagram and a fairly narrow peak at E_F for the superconducting compositions on the overdoped side (Fig. 18). Transport properties show similar scaling behaviour with similar characteristic energies but no equivalent quantitative analysis has been made. The magnetic susceptibility, Hall coefficient and thermoelectric power of the cuprates are relatively easy to measure and give meaningful results even for polycrystalline ceramics. So it should be quite easy to extend the analyses reviewed here to other families of cuprate superconductors (including materials with the highest values of T_c which are not always completely phase pure) and verify that they obey the same empirical laws found for LSCO and YBCO single crystals. This will provide a large coherent set of data which should help theorists decide on the most appropriate model for the normal state and hence for the pairing mechanism. Although we find that our results may be expressed in terms of an energy-dependent density of states for fermion quasi-particles we emphasise that this does not mean that electron-electron correlations are unimportant. Furthermore there are situations in theoretical solid state physics where interacting bosons, with slightly non-ideal commutation relations, do behave as fermions [74].

Acknowledgments

We are grateful to N. Athanassopoulou, A. Carrington, I.R. Fisher, N.E. Hussey, J.D. Johnson, W.Y. Liang, A.P. Mackenzie, K. A. Mirza, P.S.I.P.N. de Silva, J.L. Tallon, J.M. Wade and D.J.C. Walker for their contributions to the work described here.

References

[1] Gao L. *et al.*, *Phys.Rev.* **B50** (1994) 4260-4263.
[2] Hardy W.N., Bonn D.A., Morgan D.C., Liang R. and Zhang K., *Phys. Rev. Lett.* **70** (1993) 3999-4002.
[3] For example Panagopoulos C., Cooper J.R., Peacock G. B., Gameson I., Edwards P.P., Schmidbauer W. and Hodby J.W., *Phys. Rev.* **B53** (1996) 2999-3002.
[4] For a review see Annett J., Goldenfeld N. and Leggett A.J., in "Physical Properties of High Temperature Superconductors", Vol. 5, D.M. Ginsberg Ed. (World Scientific, Singapore 1996).
[5] Kirtley J.R. *et al.*, *Nature* **373** (1995) 225-228.

[6] Birgenau R.J. and Shirane G., in "Physical Properties of High Temperature Superconductors", Vol. 1, D.M. Ginsberg Ed. (World Scientific, Singapore, 1989).
[7] Rossat-Mignod J., Regnault L.P., Vettier C., Burlet P., Henry J.Y. and Lapertot G., *Physica B* **169** (1991) 58-65.
[8] Loram J.W., Mirza K.A., Cooper J.R., Athanassopoulou N. and Liang W.Y., Thermodynamic Evidence on the Superconducting and Normal State Energy Gaps in $La_{2-x}Sr_xCuO_4$, 10th Anniversary High T_c Workshop (Houston 12-16 March 1996).
[9] Loram J.W., Mirza K.A., Cooper J.R. and Liang W.Y., *Phys. Rev. Lett.* **71** (1993) 1740-1743.
[10] Tallon J.L., *Physica C* **176** (1991) 547-550.
[11] Carrington A., Walker D.J.C., Mackenzie A.P. and Cooper J.R., *Phys. Rev.* **B48** (1993) 13051-13059.
[12] Fukuzumi Y., Mizuhashi K., Takenaka K. and Uchida S., *Phys. Rev. Lett.* **76** (1996) 684-687.
[13] Kimura T. *et al., Phys. Rev.* **B53** (1996) 8733-8742.
[14] Batlogg B., Hwang H.W., Takagi H., Cava R.J., Kao H.L. and Kwo J., *Physica C* **235-240** (1994) 130-133.
[15] Carrington A., An Experimental Study of the Hall Effect and Magnetoresistance of High T_c Oxide Superconductors, Ph.D thesis (University of Cambridge, 1993).
[16] Gabay M. and Lederer P., *Phys. Rev.* **B47** (1993) 14462-14466.
[17] Bucher B, Karpinski J., Kaldis E. and Wachter P., *Phys. Rev. Lett.* **70** (1993) 2012-2015.
[18] Ito T., Takenaka K. and Uchida S., *Phys. Rev. Lett.* **70** (1993) 3995-3998.
[19] Wuyts B., Moshchalkov V.V. and Bruynseraede Y., *Phys. Rev.* **B53** (1996) 9418-9432.
[20] Cooper J.R., Obertelli S.D., Carrington A. and Loram J.W., *Phys. Rev.* **B44** (1991) 12086-12089.
[21] Takagi H., Ido T., Ishibashi S., Uota M., Uchida S. and Tokura Y., *Phys. Rev.* **B40** (1989) 2254-2261.
[22] Clayhold J., Hagen S., Wang Z.Z., Ong N.P., Tarascon J.M. and Barboux P., *Phys. Rev.* **B39** (1989) 777-780.
[23] Liu R.S., Edwards P.P., Huang Y.T., Wu S.F. and Wu P.T., *J. Sol. State Chem.* **86** (1990) 334-339.
[24] Obertelli S.D., Cooper J.R. and Tallon J.L., *Phys. Rev.* **B40** (1992) 14928-14931.
[25] Kubo Y., Shimakawa Y., Manako T. and Igarashi H., *Phys. Rev.* **B43** (1991) 7875-7882.
[26] Presland M.R., Tallon J.L., Buckley R., Liu R.S. and Flower N., *Physica C* **176** (1991) 95-105.
[27] Uchida S., Takenaka K. and Tamasaku K., preprint (1996).
[28] Wuyts B., Osquiguil E., Maenhoudt M., Libbrecht S., Gao Z.X. and Bruynseraede Y., *Phys. Rev.* **B47** (1993) 5512-5515.
[29] Jones E.C. *et al., Phys. Rev.* **B47** (1993) 8986-8995.
[30] Chien T.R., Wang Z.Z. and Ong N.P., *Phys. Rev. Lett.* **67** (1991) 2088-2091.
[31] Anderson P.W., *Phys. Rev. Lett.* **67** (1991) 2092-2095.
[32] Fisher I.R., Wagner G. and Cooper J.R. (unpublished)
[33] Kendziora C., Mandrus D., Mihaly M. and Forro L., *Phys. Rev.* **B46** (1992) 14927-14300.
[34] Mandrus D., Forro L., Kendzoria C. and Mihaly L., *Phys. Rev.* **B44** (1991) 2418-2422.
[35] Carrington A. and Cooper J.R., *Physica C* **219** (1994) 119-122.
[36] Cohn J.L., Skelton E.F., Wolf S.A. and Liu J.Z., *Phys. Rev.* **B45** (1992) 13140-13143.
[37] Loram J.W., Mirza K.A., Cooper J.R., Athanassopoulou N. and Liang W.Y., Submitted to *Phys. Rev. B* (June 1995).

[38] Cooper J.R., Mace B., Foessel L. and de Silva P.S.I.P.N. (unpublished). Ni data from reference [22].
[39] For example Pickett W.E., Krakauer H., Cohen R.E. and Singh D.J., *Science* **255** (1992) 46-55.
[40] For example Pennington C.H. and Slichter C.P., in "Physical Properties of High Temperature Superconductors", Vol. 2, D.M. Ginsberg Ed. (World Scientific, Singapore, 1990).
[41] Cooper J.R. and Carrington A., "A Simple Physical Picture for the Thermoelectric Power and Hall Effect of High T_c Superconductors'", 5th International Symposium on Superconductivity (Kobe, Japan, 16-19 November, 1992) Y. Bando and H. Yamauchi Eds. (Springer-Verlag Tokyo, 1993) pp. 95-100.
[42] Pines D., *Physica C* **235** (1994) 113-121.
[43] Stojkovic B.P. and Pines D., *Phys. Rev. Lett.* **76** (1996) 811-814.
[44] Lercher M.J. and Wheatley J.M., *Phys. Rev.* **B52** (1995) 7038-7041.
[45] Takigawa M., Copper and Oxygen NMR Studies on the Magnetic Properties of $YBa_2Cu_3O_{7-y}$ in Dynamics of Magnetic Fluctuations in High Temperature Superconductors, G. Reiter, P. Horsch and G.C. Psaltakis Eds. (Plenum Press, N.Y. 1991) pp. 61-71.
[46] Berthier C., Berthier Y., Butaud P., Horvatic M., Kitaoka Y. and Segransan P., ^{17}O and ^{63}Cu NMR Investigation of Spin Fluctuations in High T_c Superconducting Oxides, *ibid.* pp. 73-85.
[47] Horvatic M., Berthier C., Berthier Y., Segransan P., Butaud P., Clark W.G., Gillet J.A. and Henry J.Y., *Phys. Rev.* **B48** (1993) 13848-13864.
[48] Alloul H., Ohno T. and Mendels P., *Phys. Rev. Lett.* **63** (1989) 1700-1703.
[49] Lee P.A. *et al.*, *Comm. Cond. Matt. Phys.* **12** (1986) 99.
[50] Emery V.J. and Kivelson S.A., *Nature* **374** (1995) 434-437.
[51] Imai T., Slichter C.P., Yoshimura K. and Kosuge K., *Phys. Rev. Lett.* **70** (1993) 1002-1005.
[52] Suzumura Y., Hasegawa Y. and Fukuyama H., *J. Phys. Soc. Jpn* **57** (1988) 2768-2778.
[53] Zhang F.C., Gros C., Rice T.M. and Shiba H., *Supercon. Sci. Technol.* **1** (1988) 36-46.
[54] For example Altshuler B.L., Aronov A.G., Khmelnitskii D.E. and Larkin A.I., Coherent Effects in Disordered Conductors in "Quantum Theory of Solids", I.M. Lifshitz Ed. (Mir Publishers, Moscow, 1982)
[55] Ando Y., Boebinger G.S., Passner A., Kimura T. and Kishio K., *Phys. Rev. Lett.* **75** (1995) 4662-4665.
[56] Loram J.W., Mirza K.A. and Freeman P.F., *Physica C* **171** (1990) 243-252.
[57] Ishida K., Kitaoka Y., Nogata N., Kamino T., Asayama K., Cooper J.R. and Athanassopoulou N., *J. Phys. Soc. Jpn* **62** (1993) 2803-2816.
[58] Janossy A., Cooper J.R., Brunel L-C. and Carrington A., *Phys. Rev.* **B50** (1994) 3442-3445.
[59] Zagoulaev S., Monod P. and Jegoudez J., *Phys. Rev.* **B52** (1995) 10474-10487.
[60] Xiang T. and Wheatley J.M., *Phys. Rev.* **B51** (1995) 11721-11727.
[61] Xiao G., Cieplak M.Z. and Chien C.L., *Phys. Rev.* B42 (1990) 240-243.
[62] Zagoulaev S., Monod P. and Jegoudez J., *Physica C* **259** (1996) 271-279.
[63] Athanassopoulou N., Effect of Cation Substitution on the Physical Properties of the High Temperature Superconductor $YBa_2Cu_3O_{7-\delta}$, Ph.D Thesis (University of Cambridge, 1994).
[64] Cooper J.R., *Supercond. Sci. Technol.* **4** (1991) S181-183.
[65] Mirza K.A., Loram J.W. and Cooper J.R., *Physica C* **235** (1994) 1771-1772.
[66] Alloul H., Mendels P., Casalta H., Marucco J.F. and Arabski J., *Phys. Rev. Lett.* **67** (1991) 3140-3143.

[67] Cooper J.R., Obertelli S.D., Freeman P.A., Zheng D.N., Loram J.W. and Liang W.Y., *Supercond. Sci. Technol.* **4** (1991) S277-279.
[68] Walker D.J.C., Mackenzie A.P. and Cooper J.R., *Phys. Rev.* **B51** (1995) 15653-15656.
[69] Walker D.J.C., Mackenzie A.P. and Cooper J.R., *Physica C* **235-240** (1994) 1335-1336.
[70] Walker D.J.C., Magnetotransport Properties as a Function of Oxygen and Zinc Doping in Laser Ablated Thin Films of $YBa_2Cu_3O_{7-\delta}$, Ph.D Thesis (University of Cambridge, 1994).
[71] Carrington A., Mackenzie A.P., Lin C.T. and Cooper J.R., *Phys. Rev. Lett.* **69** (1992) 2855-2858.
[72] Tallon J.L., Cooper J.R., de Silva P.S.I.P.N., Williams G.V.M. and Loram J.W., *Phys. Rev. Lett.* **75** (1996) 4114-4117.
[73] Hwang H.W. *et al.*, *Phys. Rev. Lett.* **72** (1994) 2636-2639.
[74] For example: Lutzenko I. and Zhedanov A., *Phys. Rev. Lett.* **74** (1995) 3507-3510.